The 8th European Congress on Computational Methods in Applied Sciences and Engineering
ECCOMAS Congress 2022
5 – 9 June 2022, Oslo, Norway

Numerical investigation of hydrogen self-ignition and deflagration-to-detonation phenomena using automated meshing approach and detailed chemistry

MARIUS G. COJOCARU[†], LORENZO SUFRÀ[†] AND PIETRO SCIENZA[†]

[†] Convergent Science GmbH, Hauptstrasse 10, 4040 Linz, Austria,
email: gabriel.cojocaru@convergecfd.com and https://convergecfd.com/

Key words: Hydrogen Safety, Self-Ignition, Deflagration-to-Detonation Transition.

Abstract. Computational fluid dynamics (CFD) plays a critical role in designing safe storage and transport systems for hydrogen. Fine mesh resolution and detailed chemistry are essential for the accurate prediction of self-ignition and deflagration-to-detonation (DDT) in hydrogen-air mixtures. However, simulating H2 venting and explosion in real-life scenarios (e.g., with complex obstacle shapes and a large computational domain) involves tedious meshing effort and several mesh iterations to capture flame and shock locations. This paper addresses these challenges by assessing the capability of a detailed-chemistry approach combined with automated meshing based on a cut-cell technique and Adaptive Mesh Refinement (AMR).

Furthermore, three different turbulence-chemistry interaction modelling approaches are compared for self-ignition and DDT scenarios: a homogeneous reactor model, an eddy dissipation model, and a flame thickening approach.

1 INTRODUCTION

The growing interest in hydrogen as a viable source of energy for propulsion calls for particular care not only for the production process, but also for the design and assessment of safety systems and hazardous scenarios. Specifically, the design of storage units for hydrogen must account for its high volatility and flammability, along with its ability to release a large amount of energy by reacting with oxygen at ambient conditions. CFD is crucial to the design of hydrogen storage and transportation systems since it offers a relatively inexpensive, reliable, and safe approach compared to testing.

Baraldi et al. [15] defined the key benchmark cases and criteria to assess CFD accuracy for hydrogen safety scenarios in the framework of "Support to Safety aNAlysis of Hydrogen and Fuel Cell Technologies" (SUSANA) European Project, considering self-ignition jets, deflagration and detonation events. Rudy et al. [14] studied numerically the ignition process of H2 jets in air, while Halouane et al. [16] performed CFD analysis on the ENACCEF deflagration test case using Large Eddy Simulation (LES) and the Eddy Dissipation Model (EDM). In a similar framework, both Ettner et al. [3] and Weng et al. [2] investigated the DDT process in an obstructed channel.

Given the key role of CFD in the hydrogen safety assessment, and the strong interest in deeply understanding the physics that leads to hazardous scenarios, the present study proposes a detailed-chemistry approach in the framework of a fully automated Cartesian mesh generation procedure based on a cut-cell technique along with the use of AMR.

Two configurations are studied. First, a set of experiments are modelled numerically to

evaluate the conditions in which hydrogen stored in high-pressure vessels can self-ignite as it exits a narrow tube [1, 14]. Second, a numerical investigation is configured to replicate experimental investigations on DDT of hydrogen within enclosures [2, 3]. The effects of homogenous and inhomogeneous gas distribution conditions and buoyancy effects on DDT are considered.

2. TEST CASES DESCRIPTION

2.1 Self-ignition case study

The self-ignition case study is based on the works of Golub et al. [1], which were presented again in a similar study by Rudy et al. [14]. The case consists of hydrogen stored in a high-pressure tank that is being released through a long and narrow tube into the atmosphere. Autoignition has been observed for the considered tube diameter, length, and tank pressures based on 1500 K and 10^{-4} H2O mass fraction thresholds. Geometry and dimensions are shown in Figure 1. The ignition for the given configuration happens first near the wall and then propagates towards the center of the tube to occupy the full tube's cross-section as the shock wave travels towards the atmosphere. Golub et al. [1] have identified that self-ignition first occurs at tank pressures above 77 atm. There is no ignition reported at a tank pressure of 64 atm, while ignition is always reported at a tank pressure of 96 atm. For quantitative comparison to the experiment, the axial position of the autoignition is compared.

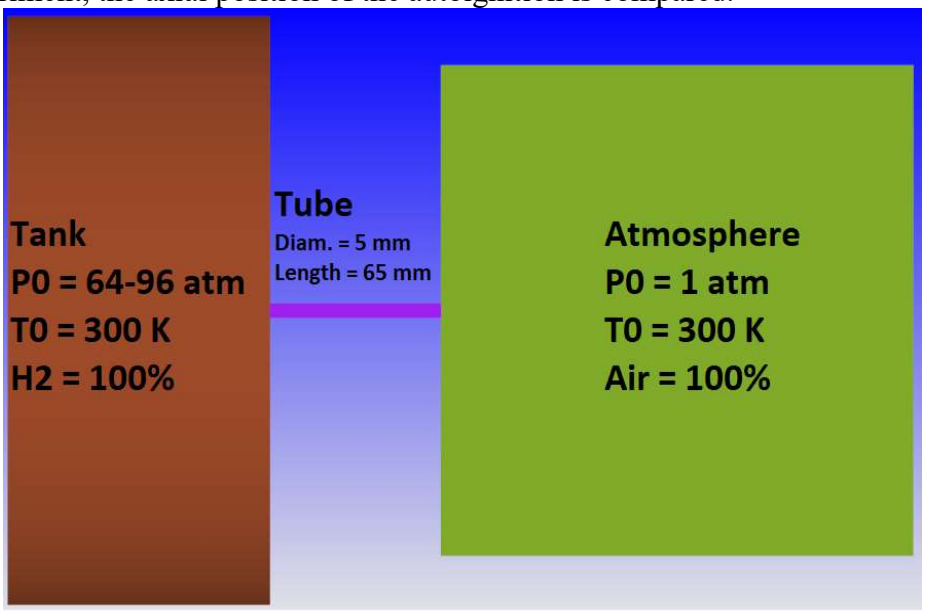

Figure 1: Self-ignition test case

2.2 Deflagration-to-detonation transition case study

The DDT case study is based on the works of Wang and Wen [2] and Ettner [3]. The case consists of an enclosed channel of size 5400mm x 60mm x 300mm and it includes 7 rows of obstacles. The ignition source is located at the center of the left-most wall as shown in **Figure 2**. The first obstacle is located at a distance of 250 mm from the ignition source and the

following ones are spaced 300 mm apart. To reach a blockage ratio of 60%, each obstacle has a height of 18 mm and a width of 12 mm. Simulations were run for different volumetric concentrations of hydrogen, namely 20% and 30%, in both homogeneous and inhomogeneous conditions across the channel's height, as shown in **Figure 3**. The homogeneous 30% concentration of hydrogen can be assumed to be close to stoichiometric, while the homogeneous 20% is considered to be lean. On the other hand, the inhomogeneous ones show a concentration gradient from very lean (close to the floor of the channel) to rich (towards the ceiling), keeping an average concentration of 20% and 30%, respectively. This creates different flame front propagation speeds in the channel. For example, the 20% inhomogeneous case has conditions for a delayed transition to detonation, while the 20% homogeneous case does not transition to detonation at all. For all configurations, the flame tip velocity versus flame tip position is reported.

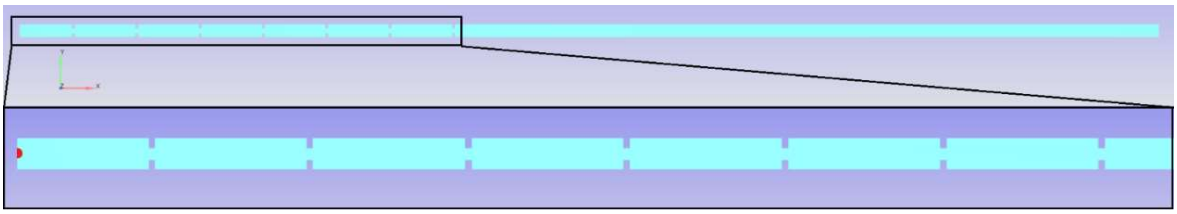

Figure 2: Deflagration-to-Detonation Transition test case

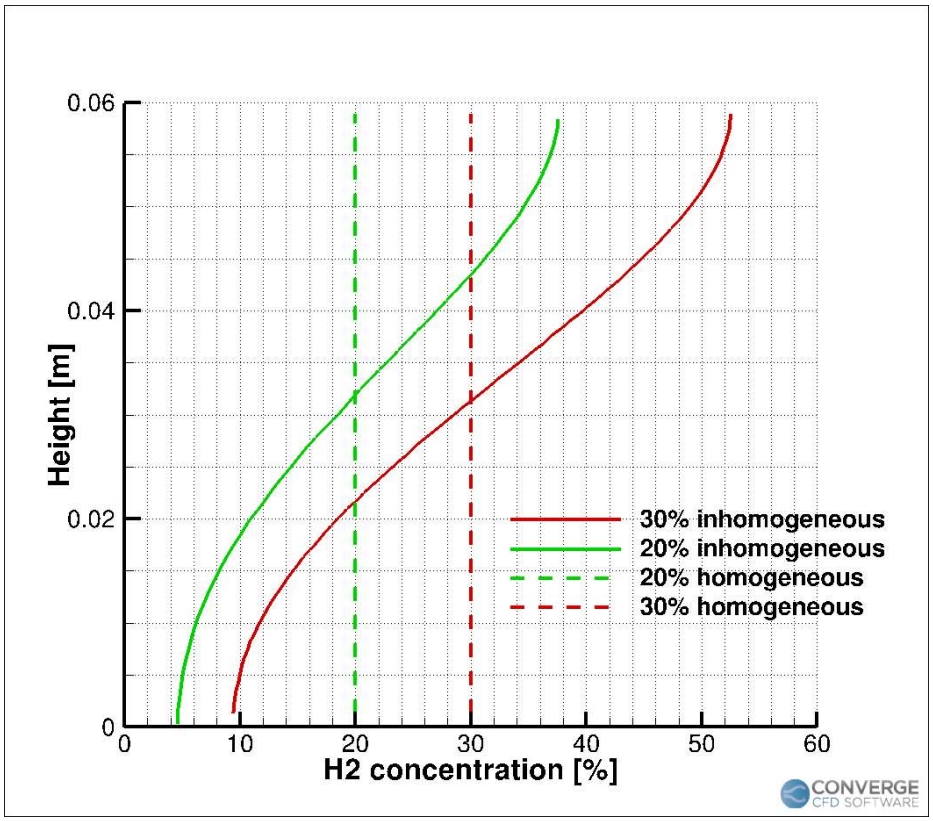

Figure 3: H_2 volumetric concentration across the channel height

3. CFD MODEL SETUP

In this work, we used CONVERGE [10] version 3.0.25 for all simulations. A fully compressible form of the Navier-Stokes equations are solved using either a URANS (Unsteady Reynolds-Averaged Navier-Stokes) approach with the well-known two-equation realizable k-ε model or an LES approach with the dynamic structure model. The transport equations are coupled with the real gas Redlich-Kwong equation of state. A second-order MUSCL (Monotonic Upstream-centered Scheme for Conservation Laws) spatial discretization scheme based on the min-mod limiter was employed for the convective fluxes. A modified PISO (Pressure-Implicit with Splitting of Operators) algorithm was used to solve the pressure-velocity coupling, while the checker-boarding effect of the pressure-velocity coupling on collocated grids was mitigated through the use of the Rhie-Chow interpolation scheme. Further details on the numerical models can be found in [12].

At runtime, the solver performs automated mesh generation based on a modified Cartesian cut-cell approach. The mesh is adapted through the AMR technique, which introduces local on-the-fly grid refinements where gradients of selected variables exceed their user-defined thresholds. This feature helps the user to reduce or even completely remove the mesh generation iterations, particularly in cases dominated by strong gradients (e.g., shocks and flame fronts) and with a highly transient nature, such as DDT phenomena.

A local boundary layer mesh is inflated from the channel walls to ensure a y^+ of about 30 for the self-ignition case as shown in **Figure 4**, while specific refinement is applied to the ignition source and the obstacle boundaries in the DDT model, with cell sizes ranging from 2.8e-3 m to 4.4e-5 m (**Figure 3**). AMR is applied to velocity and temperature in both cases.

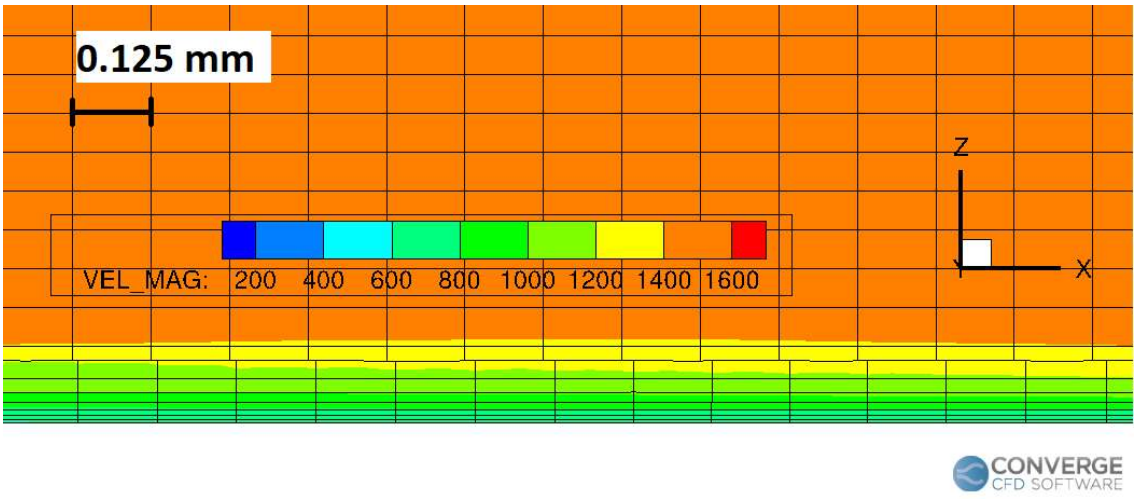

Figure 4: Self-Ignition near-wall mesh resolution.

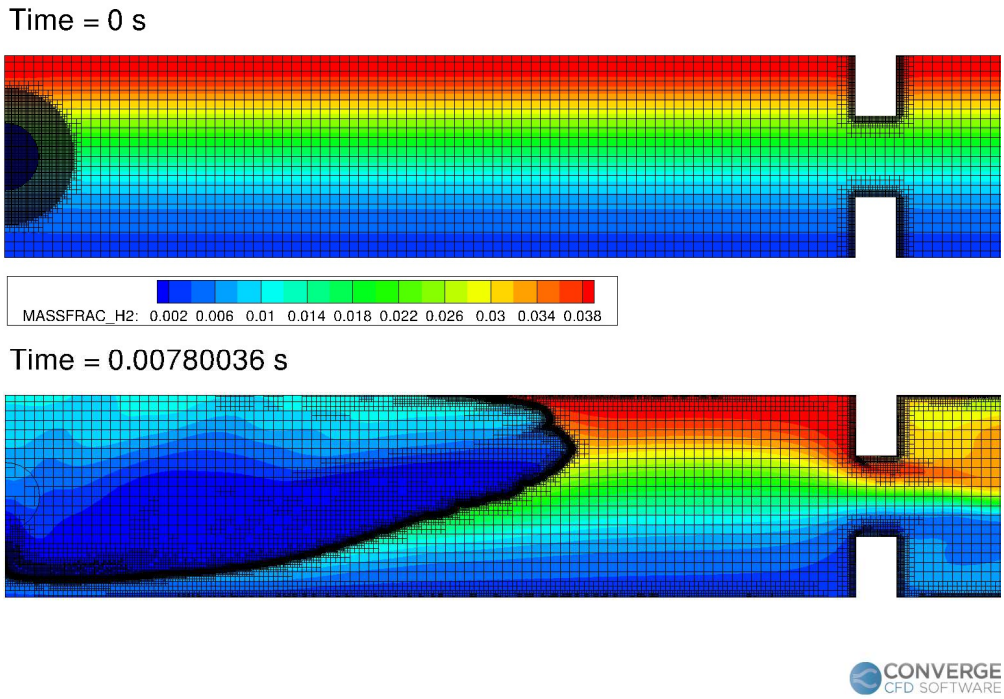

Figure 5: DDT mesh details, inhomogeneous 30% vol. case.

3.1 Combustion modelling

The two scenarios studied involve different fuel-oxidizer mixing conditions. While fully premixed or stratified mixtures are considered in the DDT case, where the flame propagation is initiated through a spark, the self-ignition scenario considers a non-premixed mixture. It is important to properly capture mixing, ignition, and flame propagation in these different configurations.

For this purpose, we compare results from two models of chemical kinetics: the SAGE homogeneous reactor model [11] and the EDM. SAGE computes reaction rates by solving an associated system of ordinary differential equations derived from the Arrhenius equation, whose coefficients are tabulated in a detailed reaction mechanism. The reaction rates are introduced in the CFD transport equations as source terms. For the URANS approach, the turbulence-chemistry interaction is modelled via the turbulent diffusivity terms in species transport equations. In the LES framework, a thickened flame model (TFM) is employed to ensure that the flame is well resolved. The TFM artificially increases the flame thickness by scaling the diffusivity while reducing the reaction source term for species, thus preserving the laminar flamespeed. The TFM in CONVERGE is coupled to AMR, allowing a fixed number of grid points to be always maintained in the thickened flame. Additional wrinkling and efficiency function models are applied to account for sub-grid scale wrinkling of the flame.

The EDM is based on the assumption that reactions are happening at a scale that is based on the turbulence properties and the reaction rate is controlled by the turbulent mixing itself. A one-step chemical kinetics reaction is used to express the chemical equilibrium and the Arrhenius coefficients. In this study, EDM is applied with URANS.

Both SAGE detailed chemistry (with and without TFM) and EDM have been tested and compared for the DDT scenario, while only SAGE has been employed in the self-ignition case.

3.2 Reaction mechanisms

Two detailed reaction mechanisms, O'Connaire [9] and Hong [4, 8], have been considered and compared for the SAGE detailed chemistry simulations.

Table 1: Extract of reaction mechanism from Hong [4, 8]

Reaction Number	Reaction	A_i [cm, g, s]	β_i [-]	E_i [cal./mol]
1	H+O2=O+OH	1.04E+14	0	1.5286E+04
2	H+O2(+M) =HO2(+M)	5.59E+13	0.2	0.0
	LOW	2.65E+19	-1.3	0.0
	TROE/ 0.7 1.0E-30 1.0E+30 1.0E+30/			
	H2/2.5000/H2O/0.0000/H2O2/12.0000/AR/0.0000/O2/0.0000/			
	H+O2(+AR) =HO2(+AR)	5.59E+13	0.2	0.0
	LOW	6.81E+18	-1.2	0.0
	TROE/ 0.7 1.0E-30 1.0E+30 1.0E+30/			
	H+O2(+O2) =HO2(+O2)	5.59E+13	0.2	0.0
	LOW	5.69E+18	-1.1	0.0
	TROE/ 0.7 1.0E-30 1.0E+30 1.0E+30/			
	H+O2(+H2O) =HO2(+H2O)	5.59E+13	0.2	0.0
	LOW	3.7E+19	-1.0	0.0
	TROE/ 0.8 1.0E-30 1.0E+30 1.0E+30/			
3	H2O2(+M) =2OH(+M)	8.59E+14	0.0	4.856E+04
	LOW	9.55E+15	0.0	4.2203E+04
	TROE/ 1.0 1.0E-10 1.0E+10 1.0E+10/			
	H2/2.5000/H2O/15.0000/H2O2/15.0000/N2/1.5000/AR/1.0000/			
4	OH+H2O2=HO2+H2O	7.586E+13	0.0	7.269E+03
	OH+H2O2=HO2+H2O	1.738E+12	0.0	3.18E+02
5	OH+HO2=H2O+O2	2.89E+13	0.0	-5.0E+02
6	2HO2=O2+H2O2	1.30E+11	0.0	-1.603E+03
	2HO2=O2+H2O2	4.2E+14	0.0	1.198E+04
7	H2O+M=H+OH+M	6.06E+27	-3.31	1.2077E+05
	O2/1.5000/H2O/0.0000/N2/2.0000/H2/3.0000/			
	H2O+H2O=OH+H+H2O	1.0E+26	-2.44	1.2016E+05
8	OH+OH=H2O+O	3.57E+04	2.4	-2.111E+03

Tables 1 and 2 show extracts of the Hong [4, 8] and O'Connaire [9] detailed reaction

mechanisms, respectively. For the sake of brevity, just the first five reactions are discussed, as these are the most relevant for the applications presented in this study.

Reaction 1 represents the chain branching reaction between atomic hydrogen and molecular oxygen. This reaction acts as a limiter of the rate of hydrogen oxidation at "high temperatures" (1250 K - 2500 K). In contrast, Reaction 2 is responsible for the hydrogen oxidation rate at "low temperatures". Both of these reactions contribute to the heat release rate (HRR), which in turn feeds the gases' expansion after combustion. At "intermediate temperatures" (850 K - 1200 K), Reaction 3 is the chain branching reaction that influences ignition the most. This reaction models the thermal decomposition of hydrogen peroxide at temperatures on the order of ~ 1050 K, previously accumulated at lower temperatures in the reactive mixture. The fast decomposition leads to the formation of highly reactive hydroxyl radicals. Reaction 4 consumes the OH radical but produces hydroperoxyl HO2 radical. Both Reactions 3 and 4 are therefore are responsible for the decomposition of H2O2 into radicals. Reaction 5 (as well as 6 and 8) consumes those radicals.

The main difference between the two mechanisms comes from Reaction 1, where the pre-exponential factor, A_i, is almost double the value showed in Hong compared to O'Connaire, while the activation energy is similar; this will in turn lead to more pronounced reaction rates once high temperatures are reached. In general, for both mechanisms, Reactions 1 and 2 are more relevant for the DDT, while Reactions 2 and 3 are important for the self-ignition process. Moreover, Reaction 5 is a leading termination path for HO2 in lean conditions and is responsible for the depletion of OH and HO2 radicals. This reaction has a strong negative sensitivity on the ignition times at high pressure, as shown by Hong [10]. Machida et al. [7] have demonstrated the capability of the Hong reaction mechanism in predicting both ignition delay time and the laminar flamespeed under conditions similar to the DDT case reported here. While for self-ignition the ignition delay time is the most relevant, for DDT both ignition delay time and flamespeed play a very important role.

Table 2: Extract of reaction mechanism from O'Connaire [9]

Reaction Number	Reaction	A_i [cm, g, s]	β_i [-]	E_i [cal./mol]
1	H+O2=O+OH	1.915E+14	0	1.644E+04
	REV	5.481E+11	0.39	-2.93E+02
2	H+O2(+M) =HO2(+M)	1.475E+12	0.6	0.0
	LOW	3.48E+16	-0.411	-1.115E+03
	TROE/ 0.5 1.0E-30 1.0E+30 1.0E+100/			
	H2/1.3000/H2O/14.0000/AR/0.6700/			
3	H2O2(+M) =2OH(+M)	2.951E+14	0.0	4.843E+04
	LOW	1.202+17	0.0	4.44E+04
	TROE/ 0.5 1.0E-10 1.0E+10 1.0E+100/			
	H2/2.5000/H2O/12.0000 /AR/0.6400/			
4	OH+H2O2=HO2+H2O	5.8E+14	0.0	9.557E+03
	REV	1.066E+13	0.59	4.045E+04
	OH+H2O2=HO2+H2O	1.0E+12	0.0	0.0

Reaction Number		Reaction	A_i [cm, g, s]	β_i [-]	E_i [cal./mol]
	REV		1.838E+10	0.59	3.089E+04
5		OH+HO2=H2O+O2	2.89E+13	0.0	-4.97E+02
	REV		5.861E+13	0.24	6.908E+04

4 RESULTS AND DISCUSSION

In the following we will present and discuss the CFD results of both self-ignition and DDT. We have used detailed chemistry (SAGE, SAGE + TFM) with either the Hong or O'Connaire reaction mechanism for both test cases. We have used EDM with a single-step mechanism for DDT only. The reason for using only detailed chemical kinetics for self-ignition is that the test case and processes happen at small scales and require detailed modeling. In support of the detailed chemical kinetics, the LES Dynamic Structure Model is the more justified choice, since the chemical scales require a fine mesh, as does LES.

4.1 Self-ignition CFD study

As stated previously, the near-wall physics plays a very important role in the self-ignition case. As seen on the right side of **Figure 6**, the absence of the inlaid mesh triggers the premature ignition of hydrogen, suggested by the presence of H2O mass fraction values as high as 0.24 and temperatures above 1800 K. Looking at a snapshot of comparable time on the case with the inlaid mesh (left side of **Figure 6**), one can see that the hydrogen does not self-ignite, as predicted by the experiments [1]. Considering this, the inlaid mesh has been used for all of the results obtained and shown for the self-ignition case.

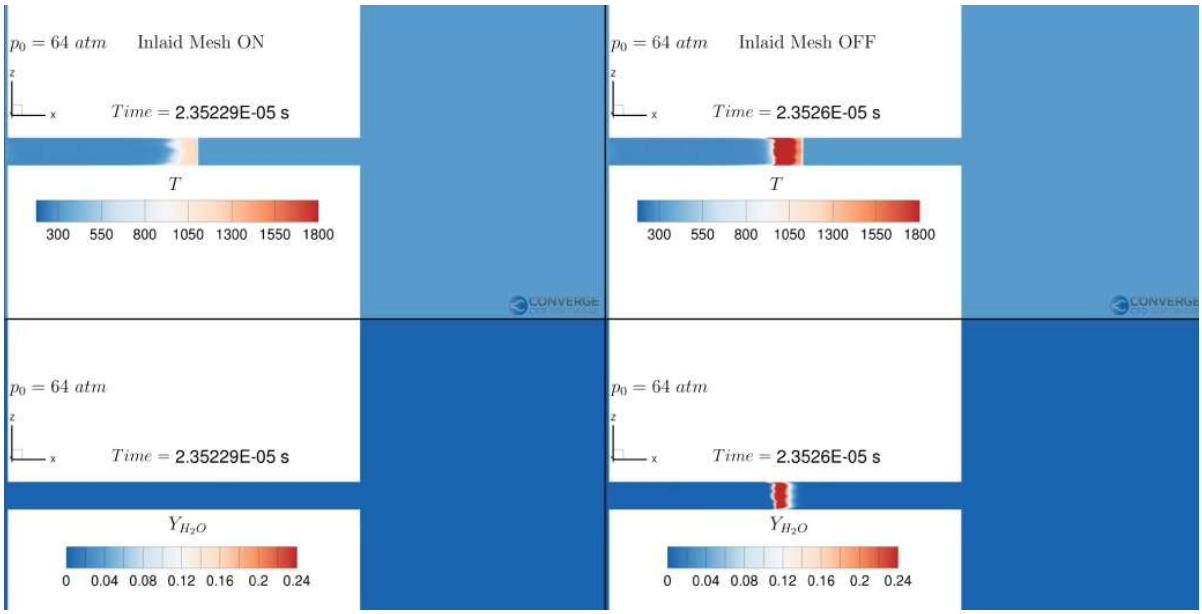

Figure 6 Self-ignition: Effect of the inlaid near-wall mesh on the prediction of ignition.

In **Table 3,** the self-ignition of CFD with the two reaction mechanisms is compared with the experimental results presented by Golub [1]. We can see that the behavior at both 64 and 96 atm are being correctly predicted, while for the 77 atm case, the numerical simulation seems to wrongly predict the autoignition as a first comparison. Taking a closer look, however, it can be noticed that ignition occurring at lower pressures and non-ignition at slightly higher ones are also reported in the experimental data [1]. This suggests that the CFD results should be reported within a band of experimental tank pressures against the upper and lower limits of the self-ignition axial position where self-ignition might or might not occur, as shown in **Figure 7**. From **Figure 7** and **8,** the Hong mechanism seems to predict self-ignition later than O'Connaire and overall, sits more comfortably within the aforementioned band.

Table 2: CFD results and experimental results [1] for ignition status.

Tank Pressure	Tube Length	Exp. [1]	CFD, Hong Mechanism	CFD, O'Connaire Mechanism
[atm.]	[mm]		Ignition status	
64	65	No	No	No
77	65	No	Yes	Yes
96	65	Yes	Yes	Yes

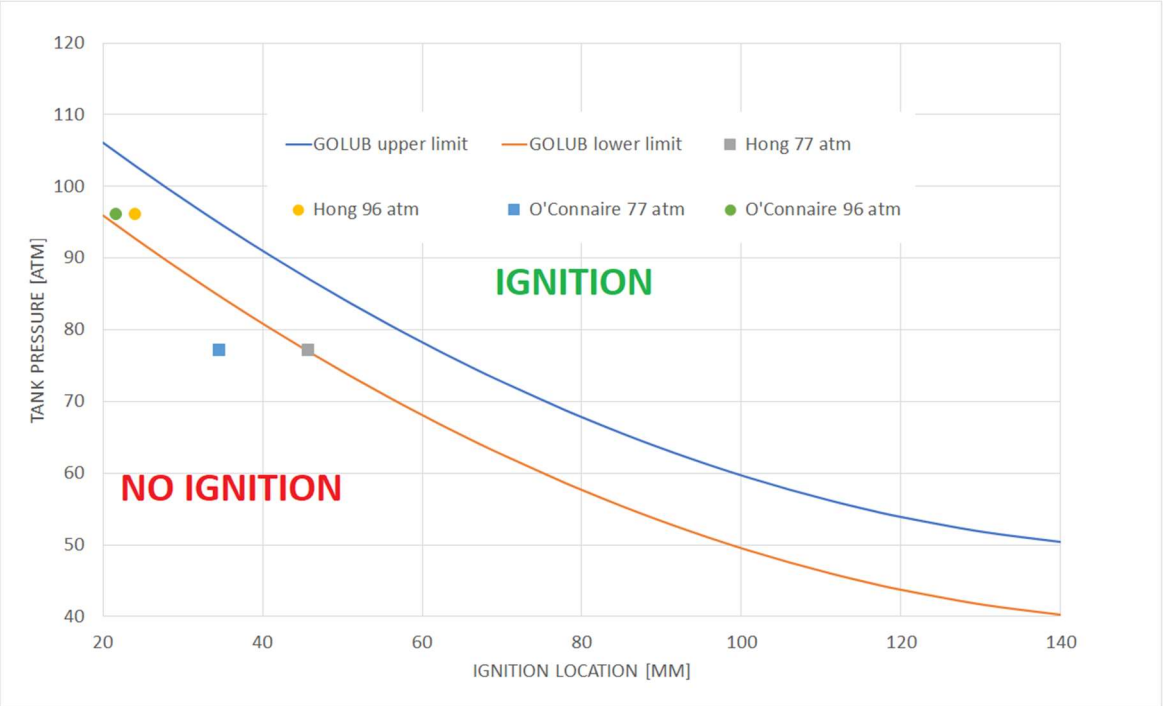

Figure 7 Self-ignition location for different tank pressures. Lines based on results reported in [1] and points based on CFD.

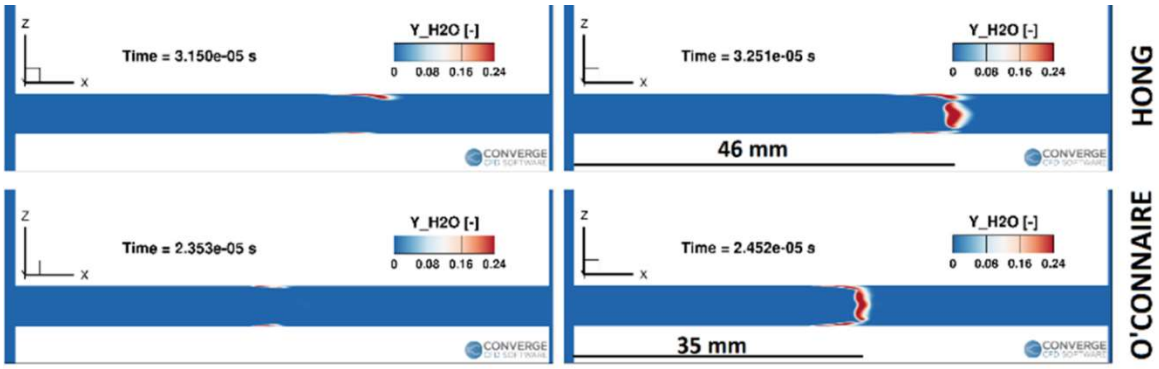

Figure 8 Self-ignition mechanism. a. Using Hong reaction mechanism b. Using O'Connaire reaction mechanisms.

4.2 Deflagration-to-detonation transition CFD study

The DDT phenomena was studied using both reaction mechanisms and also with the EDM model using a single-step reaction mechanism for hydrogen oxidation. For the 20% homogeneous and inhomogeneous hydrogen concentration, the flame tip velocity versus flame tip position CFD results are compared to experiments [3] in **Figure 9**. One can observe that for both states, all CFD models predict the behavior with fairly good accuracy, including the Chapman-Jouguet theoretical velocity, 1989 m/s. EDM seems to systematically under-predict the flame tip velocity for the first 1.5 meters. The results can, nevertheless, still be considered in an acceptable range given the simplicity of the reaction mechanism and the strong dependence on turbulence, which takes time to develop from the initial quiescent condition. It is important to note that all models compare much better to the experiment in the 20% homogeneous case that does not show any detonation. It is also encouraging that all models predict the transition to detonation at around the 3m location for the 20% inhomogeneous case.

For the 30% homogeneous and inhomogeneous hydrogen concentration, the flame tip velocity versus flame tip position CFD results are compared to experiments [3] in **Figure 10**. Once again, all models predict fairly well the flame tip velocity versus the flame tip location. The EDM model again under-predicts the flame tip velocity in the first 2 meters for both the homogeneous and inhomogeneous case, while for the inhomogeneous case it also under-predicts the flame tip velocity, even after the detonation state is achieved.

Another important observation based on the results for all DDT simulations is that the CFD model based on the O'Connaire reaction mechanism leads to results closer to the experimental ones than the cases where the Hong mechanism is used. This difference seems to come from Reaction 1, where the pre-exponential factor, A_i, is almost double in value compared to Hong, leading to more pronounced reaction rates and higher flame speed, especially in the deflagration regime.

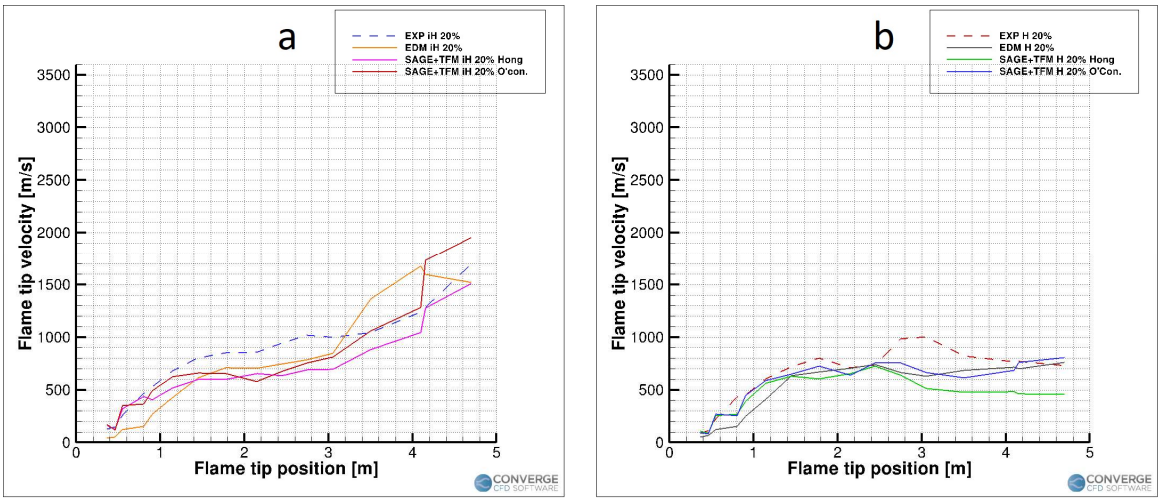

Figure 9 CFD vs experiments [3] for a. Inhomogeneous 20% hydrogen concentration; b. Homogeneous 20% hydrogen concentration.

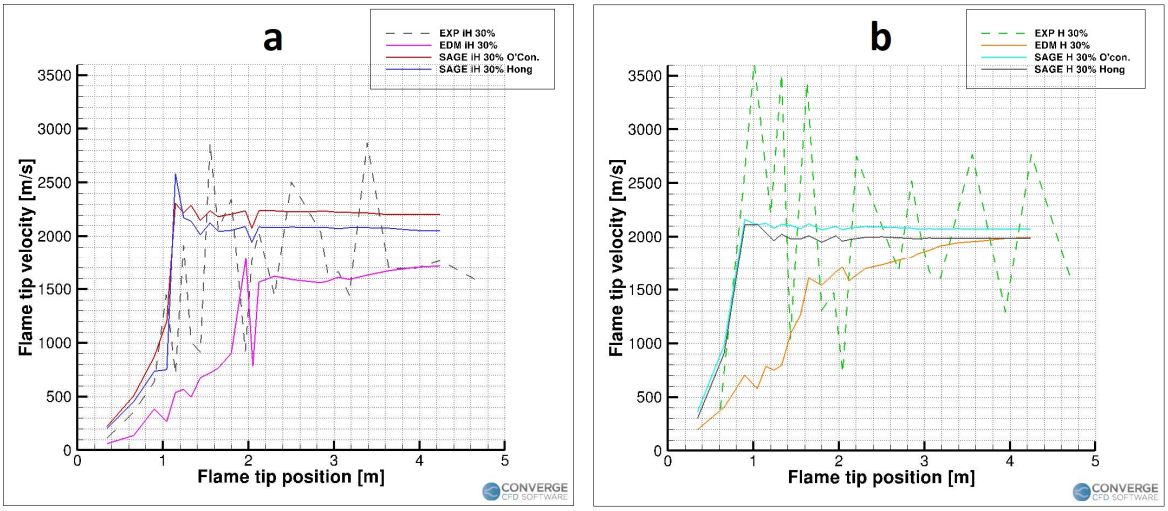

Figure 10 CFD vs experiments [3] for a. Inhomogeneous 30% hydrogen concentration; b. Homogeneous 30% hydrogen concentration.

5 CONCLUSIONS

In this work, a CFD model employing a truly automated meshing approach with Adaptive Mesh Refinement applied to self-ignition and deflagration-to-detonation scenarios has been presented. Detailed chemistry and EDM combustion modelling approaches have been employed comparing different reaction mechanisms.

The model correlates well with the experiments, especially when the detailed chemistry combustion models are employed, although showing expected sensitivity to reaction mechanisms.

It was found that the near-wall flow must be accurately captured in the self-ignition scenarios in order to capture both the viscous heating and the shock strength dampening near the wall, and the induced heating associated with it.

REFERENCES

[1] Golub, V.V. , Baklanov, D.I. , Bazhenova, T.V. , Bragin, M.V. , Golovastov, S.V., Ivanov, M.F. and Volodin, V.V.: *Shock-induced ignition of hydrogen gas during accidental or technical opening of high-pressure tanks*. Journal of Loss Prevention in the Process Industries, (2007).

[2] Wang, C.J. and Wen, J. X., *Numerical simulation of flame acceleration and deflagration-to-detonation transition in hydrogen-air mixtures with concentration gradients*, International Journal of Hydrogen Energy, Vol. 42, pp. 7657-7663, (2017).

[3] Ettner, F. *Effiziente numerische Simulation des Deagrations-Detonations-Übergangs.* Ph.D. thesis (in German), Technische Universität München, (2013).

[4] Hong, Z., Davidson, D.F., and Hanson, R.K., *An improved H2/O2 mechanism based on recent shock tube/laser absorption measurements*. Combust. Flame, 158, 633, (2011).

[5] Lindemann, F.A., Arrhenius, S., Langmuir, I., Dhar, N.R., Perrin, J., and Lewis, W.C., *Discussion on 'The Radiation Theory of Chemical Action,* Transactions of the Faraday Society, 17, 598-606, (1922)

[6] Gilbert, R.G., Luther, K., and Troe, J., *Theory of Thermal Unimolecular Reactions in the Fall-Off Range. II. Weak Collision Rate Constants,* Berichte der Bunsengesellschaft fur Physikalische Chemie, 87(2), 169-177, (1983).

[7] Machida, T., Asahara, M., Hayashi, A.K., and Tsuboi, N., *Three-Dimensional Simulation of Deflagration-to-Detonation Transition with a Detailed Chemical Reaction Model*, Combustion Science and Technology, 186:10-11, 1758-1773, (2014).

[8] Hong, Z., *An improved hydrogen/oxygen mechanism based on shock tube/laser absorption measurements*, PhD Thesis, (2010).

[9] O'Connaire, M., H. J. Curran, J. M. Simmie, W. J. Pitz, and C. K. Westbrook, *A Comprehensive Modeling Study of Hydrogen Oxidation,* Int. J. Chem. Kinet., 36:603-622, (2004)

[10] Richards, K. J., Senecal, P. K., and Pomraning, E., *CONVERGE 3.0*, Convergent Science, Madison, WI (2022).

[11] Senecal, P.K, Pomraning, E. and Richard,s K.J., 2003. *Multi-Dimensional Modeling of Direct-Injection Diesel Spray Liquid Length and Flame Lift-off Length using CFD and Parallel Detailed Chemistry*, SAE Paper 2003-01-1043, (2003).

[12] Richards, K.J., Seneca,l P.K. and Pomraning, E., *CONVERGE 3.0 Manual*, Convergent Science, Madison, WI, (2022).

[13] Heidari, A., Ferraris, S., Wen, J.X. and Tam, V.H.Y., *Numerical simulation of large-scale hydrogen detonation*, International Journal of Hydrogen Energy, 36:2538 - 2544, (2011).

[14] Rudy, W., Dąbkowski, A. and A. Teodorczyk., *Investigation into the Ignition Process of Hydrogen Jet in Air, Archivum Combustionis*, Vol. 30, no. 1-2, (2010).

[15] Baraldi, D., Melideo, D., Kotchourko, A., Ren, K., Yanex, J., Jedicke, O., Giannissi, S.G., Tolias, I.C., Venetsanos A.G., Keenan J., Makarov D., Molkov V., Slater S., Verbecke F., Duclos A., *Development Of A Model Evaluation Protocol For CFD Analysis Of Hydrogen Safety Issues – The Susana Project*, (2013).

[16] Halouane, Y. and Dehbi, A. *CFD Simulations of Premixed Hydrogen Combustion using the Eddy Dissipation and the Turbulent Flame Closure Models*, International Journal of Hydrogen Energy, 42(34), 21990-22004, (2017).